

## Effective mass suppression upon complete spin-polarization in an isotropic two-dimensional electron system

T. Gokmen, Medini Padmanabhan, K. Vakili, E. Tutuc, and M. Shayegan

*Department of Electrical Engineering, Princeton University, Princeton, New Jersey 08544, USA*

(Received 22 February 2009; revised manuscript received 20 April 2009; published 11 May 2009)

We measure the effective mass ( $m^*$ ) of interacting two-dimensional electrons confined to a 4.5-nm-wide AlAs quantum well. The electrons in this well occupy a single out-of-plane conduction-band valley with an isotropic in-plane Fermi contour. When the electrons are partially spin polarized,  $m^*$  is larger than its band value and increases as the density is reduced. However, as the system is driven to full spin-polarization via the application of a strong parallel magnetic field,  $m^*$  is suppressed down to values near or even below the band mass. Our results are consistent with the previously reported measurements on wide AlAs quantum wells where the electrons occupy an in-plane valley with an anisotropic Fermi contour and effective mass, and suggest that the effective mass suppression upon complete spin-polarization is a genuine property of interacting two-dimensional electrons.

DOI: 10.1103/PhysRevB.79.195311

PACS number(s): 73.43.Qt, 71.70.Ej, 73.50.-h

As the density of an interacting two-dimensional electron system (2DES) is reduced, the interaction strength characterized by the ratio  $r_s$  of the Coulomb energy to Fermi energy is enhanced. In low disorder, dilute 2DESs the ground-state properties are dominated by the electron-electron interaction.<sup>1</sup> In the Fermi liquid theory, interactions modify the Fermi liquid parameters<sup>2</sup> and renormalize the effective mass ( $m^*$ ) and the spin susceptibility ( $\chi^* \propto g^* m^*$ ) of the 2DES, where  $g^*$  is the Lande  $g$  factor. In particular,  $\chi^*$  and  $m^*$  are expected to be larger than the band values ( $\chi_b$  and  $m_b$ ) for large  $r_s$ .<sup>3-10</sup> Indeed, enhancements of  $\chi^*$  and  $m^*$  at large  $r_s$  are observed in various 2DESs.<sup>11-25</sup> However, in 2DESs occupying wide AlAs quantum wells (QWs) an unexpected trend is observed as the system becomes fully spin polarized:  $m^*$  is suppressed and falls to values near or below  $m_b$  even for  $r_s$  values up to 21.<sup>26</sup> A subsequent study in similar samples<sup>27</sup> revealed that the mass suppression disappears when the electrons occupy two conduction-band valleys signaling that the mass suppression is unique to single-component (fully spin and valley polarized) systems.

Here we report measurements of  $m^*$  in the partially and fully spin-polarized regime as a function of density in a 2DES where the electrons are confined to a 4.5-nm-wide AlAs QW. This 2DES is different from the 2DESs used in Ref. 26 in two important aspects: it has a very *small* layer thickness ( $<4.5$  nm) and an *isotropic* effective mass. Bulk AlAs has three equivalent, ellipsoidal conduction-band valleys at the  $X$  points of the Brillouin zone with longitudinal and transverse effective masses,  $m_l=1.05$  and  $m_t=0.205$  (in units of the free electron mass).<sup>28-31</sup> In samples of Ref. 26, the electrons are confined to either an 11 nm-, 12 nm- or 15-nm-wide AlAs QW and occupy one of the two in-plane valleys with an anisotropic Fermi contour and anisotropic band masses equal to 0.205 and 1.05, leading to  $m_b = \sqrt{m_l m_t} = 0.46$ . In contrast in the present 4.5-nm-wide AlAs QW, the electrons occupy a single out-of-plane valley with an isotropic Fermi contour and isotropic  $m_b = m_t = 0.205$ .<sup>32</sup> In spite of these differences, our main findings summarized in Fig. 1 are consistent with the study in Ref. 26: when the 2DES is partially spin polarized (open symbols),  $m^*$  is larger than its

band value and gradually increases with decreasing density. But as we fully spin polarize the 2DES by subjecting it to strong parallel magnetic fields,<sup>33</sup>  $m^*$  is suppressed down to values near the band mass (closed symbols). The two colors in Fig. 1 correspond to two different types of analyses used for the  $m^*$  determination, which we will discuss later in the paper. Given that this system is close to an ideal 2DES in the sense that it has a very small layer thickness and an isotropic Fermi contour, it appears that mass suppression upon full spin-polarization is a genuine property of interacting 2DESs.

We performed measurements on a sample grown on a GaAs (001) substrate and consisting of a 4.5-nm-wide AlAs QW, flanked by  $\text{Al}_{0.4}\text{Ga}_{0.6}\text{As}$  barriers.<sup>23,28,34</sup> We patterned the sample in a Hall bar configuration and made ohmic contacts by depositing AuGeNi and alloying in a reducing environment. Metallic front and back gates were deposited to control

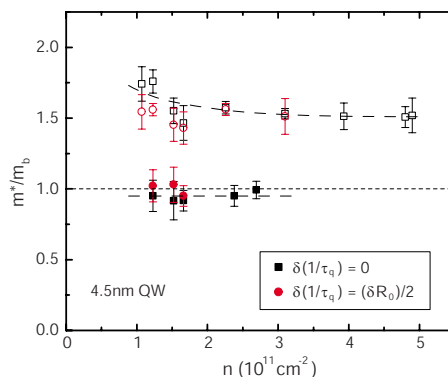


FIG. 1. (Color online) Effective mass, normalized to the band mass, measured as a function of density for a 2DES confined to a 4.5-nm-wide AlAs quantum well. Open and closed symbols represent  $m^*$  measured in partially and fully spin-polarized 2DESs, respectively. Black squares and red circles correspond to  $m^*$  values deduced either assuming a constant quantum lifetime  $\tau_q$  or that the relative temperature dependence of  $\tau_q$  is half the size of the relative temperature dependence of the background resistance, respectively. Each data point represents  $m^*$  averaged over different Landau level filling factors,  $\nu$ , and the error bars include the variation of  $m^*$  with  $\nu$ . The dashed curves through the data points are guides to the eye.

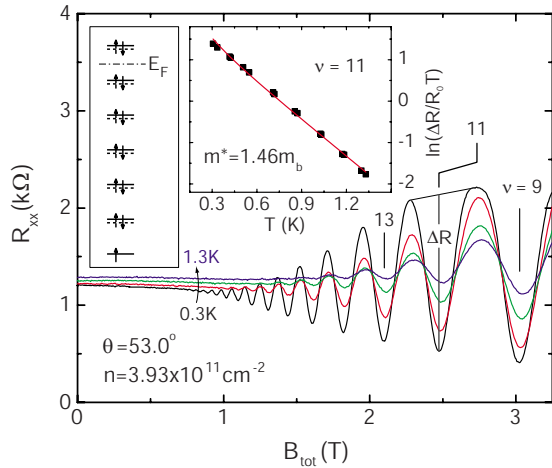


FIG. 2. (Color online) Magnetoconductance traces at a density of  $3.93 \times 10^{11} \text{ cm}^{-2}$  and  $\theta = 53.0^\circ$ . The traces were taken at  $T \cong 0.34, 0.71, 1.03,$  and  $1.30 \text{ K}$ . Insets show the energy level diagram at this tilt angle (left) and the Dingle fit at  $\nu = 11$  assuming a constant  $\tau_q$  and  $R_o$  (right).

the carrier density,  $n$ , which was determined from the frequency of Shubnikov de Haas (SdH) oscillations and from the Hall resistance. Values of  $n$  in our sample are in the range of  $1.07$  to  $4.9 \times 10^{11} \text{ cm}^{-2}$  with mobilities  $\mu = 1.4$  to  $4.9 \text{ m}^2/\text{Vs}$ . Using the AlAs dielectric constant of  $10$  and the band effective mass  $m_b = 0.205$ , our density range corresponds to  $3.1 < r_s < 6.7$ , where  $r_s$  is the ratio of the average interelectron spacing measured in units of the effective Bohr radius. The magnetoconductance measurements were performed down to a temperature ( $T$ ) of  $0.3 \text{ K}$ , and up to a magnetic field of  $31 \text{ T}$ , using low-frequency lock-in techniques. The sample was mounted on a tilting stage to allow the angle,  $\theta$ , between the normal to the sample and the magnetic field to be varied *in situ*.

To deduce  $m^*$ , we analyzed the  $T$  dependence of the strength ( $\Delta R$ ) of the SdH oscillations using the standard Dingle expression:<sup>35</sup>  $\Delta R/R_o = 8 \exp(-\pi/\omega_c \tau_q) \xi/\sinh(\xi)$ , where the factor  $\xi/\sinh(\xi)$  represents the  $T$ -induced damping ( $\xi = 2\pi^2 k_B T/\hbar \omega_c$ ) and  $\omega_c = eB_\perp/m^*$  is the cyclotron frequency,  $B_\perp$  is the perpendicular component of the magnetic field,  $R_o$  is the nonoscillatory component of the resistance near a SdH oscillation, and  $\tau_q$  is the single-particle (quantum) lifetime. We analyzed our data using two methods, each based on a different set of assumptions. First, we assumed that both  $R_o$  and  $\tau_q$  are  $T$  independent. This is the usual assumption commonly made when the  $T$  dependence of  $R_o$  is small. For our sample the  $T$  dependence of  $R_o$  is indeed weak at high densities (see, e.g., Figs. 2 and 3). At low densities, however,  $R_o$  is  $T$  dependent and, for the lowest densities,  $R_o$  changes by as much as  $60\%$  in the temperature range of our data (see, e.g., Figs. 4 and 5), implying that  $\tau_q$  can depend on  $T$ . According to a theoretical study,<sup>36</sup> for short-range scatterers, the relative  $T$ -dependent correction to  $\tau_q$  is half of the relative correction to the transport scattering time  $\tau_{tr} \propto 1/R_o$ . For long-range scatterers, the  $T$ -dependent correction to  $\tau_q$  is expected to be smaller.<sup>37</sup> In our second analysis method, we included the  $T$  dependence of  $R_o$  and assumed that the relative  $T$  dependence of  $\tau_q$  is equal to half the relative  $T$  depen-

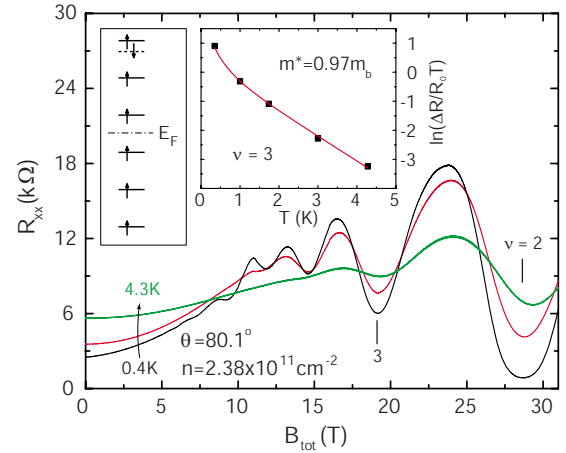


FIG. 3. (Color online) Magnetoconductance traces at a density of  $2.38 \times 10^{11} \text{ cm}^{-2}$  and  $\theta = 80.1^\circ$ . The traces were taken at  $T \cong 0.35, 0.4, 1.74,$  and  $4.28 \text{ K}$ . Insets show the energy level diagram at this tilt angle (left) and the Dingle fit at  $\nu = 3$  assuming a constant  $\tau_q$  and  $R_o$  (right).

dence of  $R_o$ .<sup>38</sup> Note that these two methods should bound the maximum error in  $m^*$  determination introduced by the  $T$  dependence of  $\tau_q$ .<sup>39</sup>

Figure 2 shows representative data for the partially spin-polarized case at a relatively high density,  $n = 3.93 \times 10^{11} \text{ cm}^{-2}$ . The angle  $\theta$  is set carefully so that the opposite spin levels are at coincidence as shown in the left inset of Fig. 2.<sup>40</sup> Consistent with this energy level diagram, in the magnetoconductance traces shown in Fig. 2 resistance minima at odd  $\nu$  are strong while the minima at even  $\nu$  are entirely absent. By fitting the amplitude of the SdH oscillations near  $\nu = 11$  to the Dingle expression and assuming  $T$  independent  $\tau_q$  and  $R_o$ , we obtain  $m^* = 1.46 m_b$  (see Fig. 2 right inset). Moreover, as illustrated in the Dingle plot in Fig. 6(a), in the whole temperature and magnetic field range the data set can be fit to the Dingle expression by assuming two constants  $\tau_q$  and  $m^*$ . Since the background resistance in this

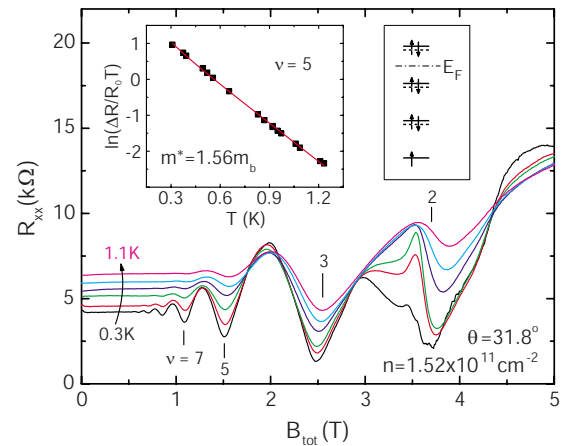


FIG. 4. (Color online) Magnetoconductance traces at a density of  $1.52 \times 10^{11} \text{ cm}^{-2}$  and  $\theta = 31.8^\circ$ . The traces were taken at  $T \cong 0.31, 0.49, 0.65, 0.83, 0.95,$  and  $1.09 \text{ K}$ . Insets show the energy level diagram at this tilt angle (right) and the Dingle fit at  $\nu = 5$  using a constant  $\tau_q$  and  $R_o$  (left).

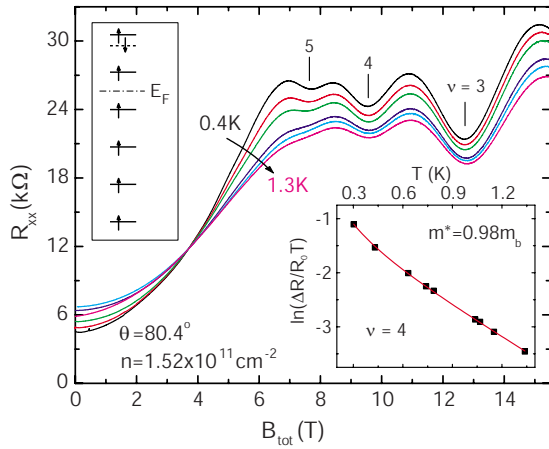


FIG. 5. (Color online) Magnetoconductance traces for the same density as in Fig. 4 at  $\theta=80.4^\circ$ . The traces were taken at  $T \approx 0.43, 0.63, 0.78, 1.07, 1.15,$  and  $1.30$  K. Insets show the energy level diagram for this tilt angle (left) and the Dingle fit at  $\nu=4$  using a constant  $\tau_q$  and  $R_o$  (right).

case has a very small temperature dependence, our second analysis method that assumes  $T$ -dependent  $\tau_q$  and  $R_o$  yields essentially the same  $m^*$ .

In Fig. 3 we show data at the density of  $2.38 \times 10^{11} \text{ cm}^{-2}$  at a very high tilt angle,  $\theta=80.1^\circ$ . At this  $\theta$ , the magnetoconductance traces initially show a rise with magnetic field because of the loss of screening with increasing spin-polarization.<sup>41</sup> The 2DES becomes fully spin polarized above  $B_{\text{tot}} \approx 11$  T and the resistance minima at  $2 \leq \nu \leq 5$  are clearly observed. Note that at this angle, the lowest five Landau levels are spin polarized as indicated by the energy-level diagram shown in Fig. 3 left inset. To measure the fully spin polarized  $m^*$  we fit the amplitude of the SdH oscillations near  $\nu=3$  to the Dingle expression by assuming  $T$ -independent  $\tau_q$  and  $R_o$ , and we deduce  $m^* = 0.97m_b$  (see Fig. 3 right inset). As is apparent from the magnetoconductance traces, although at zero field there is a

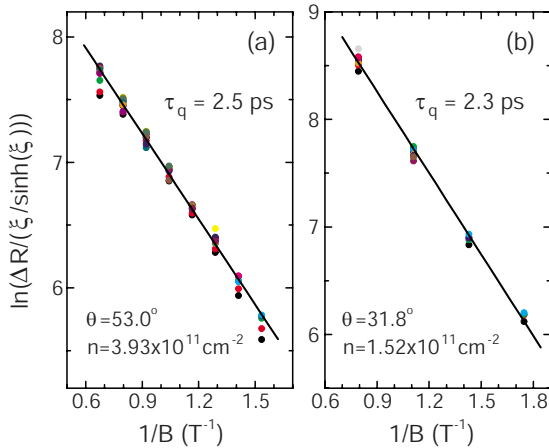


FIG. 6. (Color online) Dingle plots of  $\Delta R/[\xi/\sinh(\xi)]$  vs  $1/B$  summarizing data taken for the partially spin-polarized case for: (a) a density of  $3.93 \times 10^{11} \text{ cm}^{-2}$  in the range  $0.3 \leq T \leq 1.3$  K and  $11 \leq \nu \leq 25$ ; and (b) a density of  $1.52 \times 10^{11} \text{ cm}^{-2}$  in the range  $0.3 \leq T \leq 1.1$  K and  $5 \leq \nu \leq 11$ .

considerable change in resistance with temperature, the background resistance at the SdH oscillation near  $\nu=3$  is small. Therefore including the  $T$  dependence of  $R_o$  in the analysis does not make much difference and our first and second analysis methods give essentially identical results.

Now we present data at a lower density ( $n=1.52 \times 10^{11} \text{ cm}^{-2}$ ) where temperature dependence of the background is strong. Figure 4 shows data for the partially spin-polarized case for this density. Consistent with the energy level diagram in the right inset of Fig. 4,  $\theta$  is set to the coincidence angle so that the resistance minima at odd  $\nu$  are strong while the minima at even  $\nu$  are either entirely absent or are accompanied by a spike (e.g., at  $\nu=2$ ).<sup>42</sup> By fitting the amplitude of the SdH oscillations near  $\nu=5$  to the Dingle expression and assuming  $T$ -independent  $\tau_q$  and  $R_o$ , we obtain  $m^* = 1.56m_b$  (see Fig. 4 left inset). The Dingle plot for this data set is also shown in Fig. 6(b). It is apparent from the quality of the fit that single  $\tau_q$  and  $m^*$  can explain the whole data set in the given temperature and magnetic-field range. However, as discussed before, the quality of the fit does not justify the assumption of  $\tau_q$  being  $T$  independent. In addition, as can be seen from the magnetoconductance traces in Fig. 4,  $R_o$  changes with  $T$  as much as 50% in the indicated temperature range, implying that  $\tau_q$  can also be  $T$  dependent. Therefore, applying our second analysis method, i.e., including the  $T$  dependence of  $R_o$  and assuming a  $T$ -dependent  $\tau_q$  that changes by 25% in the same temperature range, we deduce  $m^* = 1.44m_b$ .

In Fig. 5 we show data at the same density as in Fig. 4 but at a very high tilt angle,  $\theta=80.4^\circ$ . Main features of the data are the same as in Fig. 3: magnetoconductance traces show an initial rise with magnetic field and the 2DES becomes fully spin polarized above  $B_{\text{tot}} \approx 7$  T. Filling factors  $\nu \leq 5$  are in the fully spin-polarized regime as indicated by the energy level diagram shown in Fig. 5 left inset. To measure the fully spin-polarized  $m^*$  we fit the amplitude of the SdH oscillations near  $\nu=4$  to the Dingle expression by assuming  $T$ -independent  $\tau_q$  and  $R_o$ , and we deduce  $m^* = 0.98m_b$  (see Fig. 3 right inset). As can be seen from the magnetoconductance traces, the 2DES goes through a metal-insulator transition at  $B_{\text{tot}} \approx 3.7$  T before the electrons become fully spin polarized.<sup>23</sup> The background resistance around  $\nu=4$  therefore has an insulating behavior. Again using our second method, i.e., including the  $T$  dependence of  $R_o$  and assuming a  $T$ -dependent  $\tau_q$  that is half as large as the  $T$  dependence of  $R_o$ , we deduce  $m^* = 1.11m_b$ .

We analyzed data at various  $\nu$  at several densities. Our results are summarized in Fig. 1, where each data point represents  $m^*$  averaged over different  $\nu$ , and the error bar includes the variation of  $m^*$  with  $\nu$ . The results from the first and second analysis methods are shown as black squares and red circles in Fig. 1, respectively. At high densities where the background is  $T$  independent, the two methods yield essentially identical results. However, as the density of the 2DES is lowered, the  $T$ -dependent background becomes stronger and the two methods give slightly different masses. Independently of the method we use, our conclusions remain the same: in the partially spin-polarized case<sup>43</sup>  $m^*$  is enhanced over  $m_b$  and increases with decreasing density, while for the fully spin-polarized system  $m^*$  values are clearly suppressed

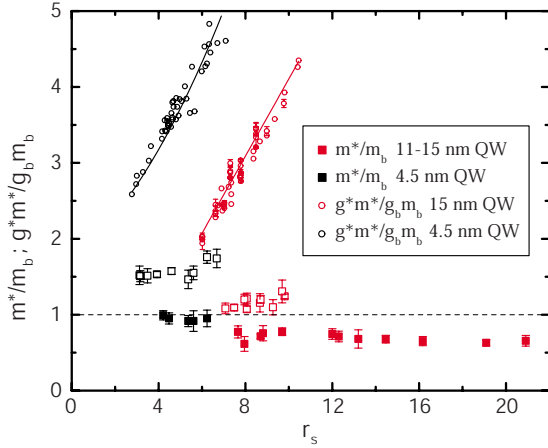


FIG. 7. (Color online) Normalized effective mass and spin susceptibilities of both narrow and wide AlAs QWs as a function of the interaction strength,  $r_s$ . Black and red circles are  $g^*m^*/g_b m_b$  of 4.5 nm- and 15-nm-wide AlAs QWs taken from Refs. 23 and 10, respectively. The thin curves through the data points are guides to the eye. Open and closed red squares are  $m^*/m_b$  for partially and fully spin-polarized system, respectively, for 11 to 15-nm-wide AlAs QWs from Ref. 26. Black squares are  $m^*/m_b$  data measured in our sample for a 4.5-nm-wide AlAs QW.

compared to the partially spin-polarized case and are very close to  $m_b$ .

As another summary plot, in Fig. 7 we show the normalized effective mass and the spin susceptibilities of both narrow and wide AlAs QWs as a function of interaction strength,  $r_s$ . Black and red circles are the normalized spin susceptibilities of 4.5 nm- and 15-nm-wide AlAs QWs, taken from Refs. 23 and 10, respectively. Open and closed red squares represent  $m^*/m_b$  for partially and fully spin-polarized system, respectively, for the wide AlAs QWs of Ref. 26. Black squares are the measured  $m^*$  data for our sample that are shown in Fig. 1.

In an ideal 2DES, the normalized values of the spin susceptibility and effective mass each should follow a universal curve as a function of  $r_s$ .<sup>3,9</sup> However nonideal factors such as finite layer thickness, anisotropy of the Fermi contour, and disorder give nonuniversal corrections. Although for high quality samples the effect of disorder is small,<sup>4,5</sup> finite layer thickness, and anisotropy of the Fermi contour modify the interaction significantly<sup>5,6,10,44</sup> and change the spin susceptibility and the effective mass renormalization. Because of the small layer thickness and isotropic Fermi contour of the electrons in narrow AlAs samples, the spin susceptibility follows very closely the predictions of quantum Monte Carlo calculations for an ideal 2D system (not shown).<sup>3,5,23,28</sup> However, for wide AlAs samples the measured susceptibilities are considerably lower than narrow AlAs samples because the strength of the Coulomb interaction is reduced by the finite layer thickness effect<sup>5,6</sup> and the anisotropy of the Fermi contour.<sup>10</sup> It is clear from the data that the partially spin-polarized masses for wide AlAs QWs are also smaller than for narrow AlAs QWs even though the  $r_s$  values are larger. Similar to the spin-susceptibility case,<sup>10</sup> the corrections to  $m^*$  due to the layer thickness and the anisotropic effective mass

are expected to give smaller  $m^*$  values in the partially spin-polarized case,<sup>6,9</sup> consistent with our data. In addition, we emphasize that the mobility of the electrons in narrow quantum wells are much lower compared to wide quantum wells because of the prevalence of the interface roughness scattering. Therefore, it is also possible that the higher disorder in narrow quantum wells is responsible for  $m^*$  being larger.<sup>4</sup> We point out that in the partially polarized case there are also some quantitative differences between our results on narrow AlAs QWs and the previous studies done on Si metal-oxide-semiconductor field-effect transistors (MOSFETs)<sup>18,19</sup> and GaAs 2DESs.<sup>24</sup> It has been reported that in GaAs 2DESs  $m^*$  has a strong  $r_s$  dependence although  $m^*$  values are much smaller compared to narrow AlAs QWs for the similar  $r_s$  range. It is likely that this discrepancy is because of the larger finite layer thickness and less disorder in 2DESs in GaAs samples. On the other hand, because of the valley degeneracy of Si-MOSFET samples, such a comparison is not valid: as shown in Ref. 27, the valley degeneracy affects the mass renormalization considerably.

In the fully polarized regime, it is natural to also expect some dependence of  $m^*$  on the layer thickness, Fermi contour anisotropy, and disorder. However, it is not clear from the data whether  $m^*$  are lower for wide AlAs samples because of nonideal factors or because these masses are measured at larger  $r_s$  values. We conclude that the mass suppression is very robust and is observed in a very wide range of  $r_s$  values and independent of sample and system parameters such as disorder, layer thickness, and anisotropy.

It is intuitively clear that the spin-polarization of the 2DES should affect the  $m^*$  renormalization since it modifies the exchange interaction. Naively, one might think that for a fully spin-polarized system the Fermi energy is doubled so the interaction is weaker compared to the spin-unpolarized case, and hence the mass for the spin-polarized case would be smaller. Although this argument gives the correct qualitative behavior of  $m^*$  for a fixed density, it does not explain why  $m^*$  for the fully polarized system stays small (near or below  $m_b$ ) even at very high  $r_s$  values. Recent theoretical work<sup>7,8</sup> has addressed the role of spin-polarization on  $m^*$  renormalization. It is reported in Ref. 7 that  $m^*$  very weakly depends on the spin-polarization for valley degenerate systems. Since in our case the 2D electrons occupy a single valley, this is not relevant to our data. The more relevant study,<sup>8</sup> which deals with a single-valley system, reports a rather strong dependence of  $m^*$  on the degree of spin-polarization. Although it is predicted in Ref. 8 that for a fully spin-polarized 2DES  $m^*$  is smaller compared to the spin-unpolarized case, there remains major qualitative discrepancies with our data. For example,  $m^*$  for a fully spin-polarized system is predicted to increase with increasing  $r_s$  and become smaller than  $m_b$  only for  $r_s < 2$ . In contrast, our data suggest that  $m^*$  stays very close to  $m_b$  even in the range  $4 < r_s < 6$ . Including the data from Ref. 26, which extends up to  $r_s \approx 21$ , the discrepancy becomes even more serious. An understanding of the magnitude and density dependence of  $m^*$  for a single component (single valley and fully spin polarized) 2DES awaits future theoretical developments.

In summary, we confirmed the observation of  $m^*$  suppres-



sion upon full spin-polarization in a system with a very small layer thickness and isotropic Fermi contour. Since this system is very close to an ideal 2DES, our data suggest that mass suppression for a single-component system is a general property of an interacting 2DES.

We thank the NSF for support. Part of this work was done at the NHMFL, Tallahassee, which is also supported by the NSF. We thank B. Tanatar and R. Asgari for discussions, and E. Palm, T. Murphy, B. Pullum, and S. Maier for assistance.

- <sup>1</sup>B. Tanatar and D. M. Ceperley, Phys. Rev. B **39**, 5005 (1989).
- <sup>2</sup>Y. Kwon, D. M. Ceperley, and R. M. Martin, Phys. Rev. B **50**, 1684 (1994).
- <sup>3</sup>C. Attaccalite, S. Moroni, P. Gori-Giorgi, and G. B. Bachelet, Phys. Rev. Lett. **88**, 256601 (2002).
- <sup>4</sup>R. Asgari, B. Davoudi, and B. Tanatar, Solid State Commun. **130**, 13 (2004).
- <sup>5</sup>S. De Palo, M. Botti, S. Moroni, and G. Senatore, Phys. Rev. Lett. **94**, 226405 (2005).
- <sup>6</sup>Y. Zhang and S. Das Sarma, Phys. Rev. B **72**, 075308 (2005).
- <sup>7</sup>S. Gangadharaiah and D. L. Maslov, Phys. Rev. Lett. **95**, 186801 (2005).
- <sup>8</sup>Y. Zhang and S. Das Sarma, Phys. Rev. Lett. **95**, 256603 (2005).
- <sup>9</sup>R. Asgari and B. Tanatar, Phys. Rev. B **74**, 075301 (2006).
- <sup>10</sup>T. Gokmen, M. Padmanabhan, E. Tutuc, M. Shayegan, S. De Palo, S. Moroni, and G. Senatore, Phys. Rev. B **76**, 233301 (2007).
- <sup>11</sup>F. F. Fang and P. J. Stiles, Phys. Rev. **174**, 823 (1968).
- <sup>12</sup>J. L. Smith and P. J. Stiles, Phys. Rev. Lett. **29**, 102 (1972).
- <sup>13</sup>T. Okamoto, K. Hosoya, S. Kawaji, and A. Yagi, Phys. Rev. Lett. **82**, 3875 (1999).
- <sup>14</sup>W. Pan, D. C. Tsui, and B. L. Draper, Phys. Rev. B **59**, 10208 (1999).
- <sup>15</sup>S. A. Vitkalov, H. Zheng, K. M. Mertes, M. P. Sarachik, and T. M. Klapwijk, Phys. Rev. Lett. **87**, 086401 (2001).
- <sup>16</sup>A. A. Shashkin, S. V. Kravchenko, V. T. Dolgoplov, and T. M. Klapwijk, Phys. Rev. Lett. **87**, 086801 (2001).
- <sup>17</sup>A. A. Shashkin, S. V. Kravchenko, V. T. Dolgoplov, and T. M. Klapwijk, Phys. Rev. B **66**, 073303 (2002).
- <sup>18</sup>V. M. Pudalov, M. E. Gershenson, H. Kojima, N. Butch, E. M. Dizhur, G. Brunthaler, A. Prinz, and G. Bauer, Phys. Rev. Lett. **88**, 196404 (2002).
- <sup>19</sup>A. A. Shashkin, Maryam Rahimi, S. Anissimova, S. V. Kravchenko, V. T. Dolgoplov, and T. M. Klapwijk, Phys. Rev. Lett. **91**, 046403 (2003).
- <sup>20</sup>J. Zhu, H. L. Stormer, L. N. Pfeiffer, K. W. Baldwin, and K. W. West, Phys. Rev. Lett. **90**, 056805 (2003).
- <sup>21</sup>O. Prus, Y. Yaish, M. Reznikov, U. Sivan, and V. Pudalov, Phys. Rev. B **67**, 205407 (2003).
- <sup>22</sup>E. Tutuc, S. Melinte, E. P. De Poortere, M. Shayegan, and R. Winkler, Phys. Rev. B **67**, 241309(R) (2003).
- <sup>23</sup>K. Vakili, Y. P. Shkolnikov, E. Tutuc, E. P. De Poortere, and M. Shayegan, Phys. Rev. Lett. **92**, 226401 (2004).
- <sup>24</sup>Y.-W. Tan, J. Zhu, H. L. Stormer, L. N. Pfeiffer, K. W. Baldwin, and K. W. West, Phys. Rev. Lett. **94**, 016405 (2005).
- <sup>25</sup>Y.-W. Tan, J. Zhu, H. L. Stormer, L. N. Pfeiffer, K. W. Baldwin, and K. W. West, Phys. Rev. B **73**, 045334 (2006).
- <sup>26</sup>M. Padmanabhan, T. Gokmen, N. C. Bishop, and M. Shayegan, Phys. Rev. Lett. **101**, 026402 (2008).
- <sup>27</sup>T. Gokmen, M. Padmanabhan, and M. Shayegan, Phys. Rev. Lett. **101**, 146405 (2008).
- <sup>28</sup>M. Shayegan, E. P. De Poortere, O. Gunawan, Y. P. Shkolnikov, E. Tutuc, and K. Vakili, Phys. Status Solidi B **243**, 3629 (2006).
- <sup>29</sup>T. S. Lay, J. J. Heremans, Y. W. Suen, M. B. Santos, K. Hirakawa, M. Shayegan, and A. Zrenner, Appl. Phys. Lett. **62**, 3120 (1993).
- <sup>30</sup>H. Momose, N. Moria, C. Hamaguchia, T. Ikaidab, H. Arimoto, and N. Miura, Physica E **4**, 286 (1999).
- <sup>31</sup>O. Gunawan, E. P. De Poortere, and M. Shayegan, Phys. Rev. B **75**, 081304(R) (2007).
- <sup>32</sup>We use  $m_b=m_t=0.205 \pm 0.005$  for the out-of-plane valley, based on values reported in different studies of either the cyclotron resonance or the ballistic transport measurements (Refs. 29–31).
- <sup>33</sup>In a 2DES with finite electron layer thickness, parallel magnetic couples to the orbital motion of the electrons and leads to an increase in  $m^*$  [T. Gokmen, M. Padmanabhan, O. Gunawan, Y. P. Shkolnikov, K. Vakili, E. P. DePoortere, and M. Shayegan, Phys. Rev. B **78**, 233306 (2008)]. However because of the very small electron layer thickness in our narrow quantum well, we expect that the mass enhancement is less than 5% even at  $B_{\parallel} = 30$  T.
- <sup>34</sup>K. Vakili, Y. P. Shkolnikov, E. Tutuc, E. P. De Poortere, M. Padmanabhan, and M. Shayegan, Appl. Phys. Lett. **89**, 172118 (2006).
- <sup>35</sup>R. B. Dingle, Proc. R. Soc. Lond. A Math. Phys. Sci. **211**, 517 (1952).
- <sup>36</sup>Y. Adamov, I. V. Gornyi, and A. D. Mirlin, Phys. Rev. B **73**, 045426 (2006).
- <sup>37</sup>S. Das Sarma (unpublished).
- <sup>38</sup>We emphasize that in all cases our data can be fit reasonably well to the Dingle expression in the whole temperature and magnetic field range by assuming two constants  $\tau_q$  and  $m^*$  (see, e.g., Fig. 6). However, this does not justify that  $\tau_q$  is independent of  $T$ ; indeed a given data set can be fit equally well to the Dingle expression with a different, fixed  $m^*$ , and a  $\tau_q$  that has some  $T$  dependence. Since  $m^*$  and the  $T$  dependence of  $\tau_q$  cannot be determined independently, in our second analysis method we use the  $T$  dependence of the background resistance to estimate the  $T$  dependence of  $1/\tau_q$  and deduce  $m^*$ .
- <sup>39</sup>Although the  $T$  dependence of  $R_o$  and  $\tau_q$  tend to cancel each other in the fitting of  $m^*$ , it is the  $T$  dependence of  $\tau_q$  that dominates since  $\tau_q$  appears inside the exponential term.
- <sup>40</sup>The partially spin-polarized masses are also reported in Ref. 23. However those masses are not deduced at the coincidence condition. Setting the coincidence condition is important because when the spin-up and spin-down levels do not overlap, the gap is smaller than the cyclotron energy and one may get artificially larger values for  $m^*$ .
- <sup>41</sup>V. T. Dolgoplov and A. Gold, JETP Lett. **71**, 27 (2000); I. F. Herbut, Phys. Rev. B **63**, 113102 (2001).

<sup>42</sup>E. P. De Poortere, E. Tutuc, S. J. Papadakis, and M. Shayegan, *Science* **290**, 1546 (2000).

<sup>43</sup>In our study, the “partially-spin-polarized” regime corresponds to spin-polarization ranging from 4% to 20%.

<sup>44</sup>In 2D systems the nonuniversal correction arising from the finite

layer thickness is a conceptually simple form factor that modifies the bare Coulomb interaction. Similarly, the Fermi contour anisotropy can be incorporated in Coulomb interaction by making a coordinate transformation that makes the Fermi surface isotropic but the interactions anisotropic.